Polarimetric X-band radar measurements of the development of precipitation observed during COPE

C. Collier[1], A. Blyth[1], L. Bennett[1], D. Dufton[1], and J. French[2]

[1] National Centre for Atmospheric Science, University of Leeds, UK; [2] University of Wyoming, USA

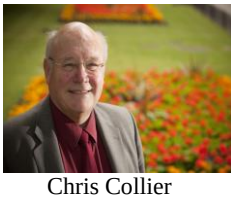

Chris Collier

1 The COPE Campaign

The COPE field campaign operated from the 3rd July to the 20th August 2013, with ground operations based in Davidstow Cornwall where the X-band polarimetric Doppler radar was located. Figure 1 shows the location of Davidstow, the Chilbolton S-band polarimetric Doppler radar and the C-band radars within the Met Office network. The Met Office Cobbacombe C-band radar was operational although not with Doppler velocity or dual polarization capability, whereas the Predannack C-band radar was not operational during COPE. The purpose of this paper is to discuss the use or benefits of the various polarization parameters produced by the X-band radar.

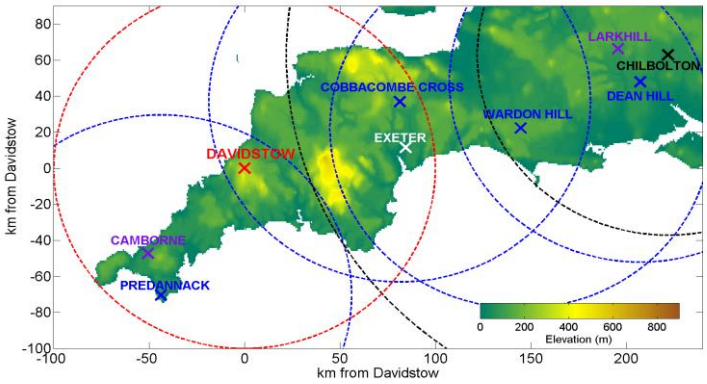

Figure 1: Layout of the radars. The red dashed circle shows the coverage of the Davidstow radar

2 The NCAS mobile radar

Ground operations included the event based deployment of a mobile, dual polarization, Doppler X-band radar with a 2.4m parabolic antenna, full technical details of which can be seen in **Table 1**. Figure 2 shows the mobile radar compared to the 25m antenna of the Chilbolton S-band radar which also operated in COPE.

Table 1: Technical specifications of SELEX Mobile Radar

Frequency	9.375 GHz	Pulse width	1 µs variable
Coaxial magnetron	Three pulse modes		
Peak transmit power	75 kW	Antenna gain	45dB
Antenna-no radome	2.4m	Scan velocity	20deg/s
PRF	Variable during COPE	Beam width	1 deg

The mobile radar operated with a scan strategy determined by current atmospheric conditions, ranging from clear air to precipitation. Most precipitation scans were dual polarisation (1000/800Hz staggered PRF) with 1 degree, 2 degrees or 3 degrees separation up to 10 elevations.

chris.collier@ncas.ac.uk

Figure 2: Left hand panel: Mobile X-band radar (2.4m diameter antenna) compared with the Chilbolton S-band radar (25m diameter antenna) at Chilbolton. Right hand panel: The mobile radar at Davidstow, Cornwall.

3. Polarization parameters

There are two ways in which hydrometeors affect polarization measurements namely (a) backscatter effects by particles located within the radar resolution volume, and (b) propagation effects by particles located between the radar resolution volume and the radar.

(a) Backscatter effects by particles located within the radar resolution volume

There are six basic backscatter variables:

1. Reflectivity factor for horizontal polarization $\mathbf{Z_{HH}}$
2. The ratio of the reflected power (or reflectivity factor) at horizontal/vertical polarization (P_{HH}/P_{VV} or Z_{HH}/Z_{VV}) called the *Differential Reflectivity* ($\mathbf{Z_{DR}}$).
3. The ratio of cross-polar power to copolar power (Φ_{VH}/Φ_{HH}) called the *Linear Depolarization Ratio* ($\mathbf{L_{DR}}$). However, the NCAS mobile radar operates in the mode of simultaneous transmission and reception of horizontally and vertically polarized waves (e.g. Doviak and Zrnic 1993). Therefore, LDR measurements are not made with the NCAS mobile radar.
4. The *correlation coefficient* between copolar horizontally and vertically polarized echo signal $\boldsymbol{\rho_{HV}\, e^{i\delta}}$ where $\boldsymbol{\delta}$ is the phase difference in H and V caused by backscattering referred to as the *differential phase upon backscatter*. This is caused by backscattering from objects within the radar resolution volume. It occurs when nonspherical hydrometeors are large enough relative to the radar wavelength such that scattering is in the Mie regime sometimes called the resonance regime (Tromel et al., 2013). Figure 7 shows that some of the hydrometeors on the 2nd August were very large (up to 6mm diameter) and likely to cause scattering in this regime.
5. The complex correlation coefficient between copolar horizontal and cross-polar (horizontal transmission) echo $E(V_{HH}{}^{*}V_{HV})$.
6. The complex correlation coefficient between copolar vertical and cross-polar (vertical transmission) echo $E(V_{HH}{}^{*}V_{HV})$.

(b) Propagation effects by particles located between the radar resolution volume and the radar

1. Attenuation of the horizontal component
2. Attenuation of the vertical component
3. *Depolarization:* Sometimes a pulse will be scattered back towards the radar in its opposite polarisation. This switch in polarisation is referred to as depolarisation. The *Degree Of Polarisation (DOP)* is a quantity used to describe the portion of an electromagnetic wave which is polarized. Galletti and Zrnic (2012) show that the DOP is related to differential reflectivity (Z_{DR}) and the copolar correlation coefficient (ρ_{hv}) when a linear receive basis is used, as follows:

$$(1 - DOP^2) = 4.Z_{DR.}\,(1 - [\rho_{hv}]^2) / [1 + Z_{DR}]^2 \qquad (1)$$

However DOP and ρ_{hv} are very similar and further consideration is necessary to ascertain whether DOP is a useful parameter or not. DOP may be of use in highlighting the bright-band as shown in Figure 3.
4. *Differential propagation phase shift* (phase difference in the returned signal for the two polarizations) Φ_{DP}. The phase of the forward scatter component depends on the wave polarization therefore, we expect the propagation phase shift (Φ) to vary as a function of polarization (e.g., horizontal, H, and vertical, V). The total measured differential propagation phase (Φ_{DP}) (sometimes called the "differential propagation phase shift) is defined as the difference between Φ_H and Φ_V: $\Phi_{DP} = [\Phi_H - \Phi_V]$. A transmitted radar wave of a given polarization interacts with a medium containing oriented non-spherical hydrometeors (e.g., raindrops), the resultant wave at some point is phase shifted. This phase shifted "effective" wave is due to a superposition of both the forward scattered and transmitted wave phases (which have different origins and hence different phase angles). Unlike ZDR, differential phase shift is also *dependent upon particle concentration*.

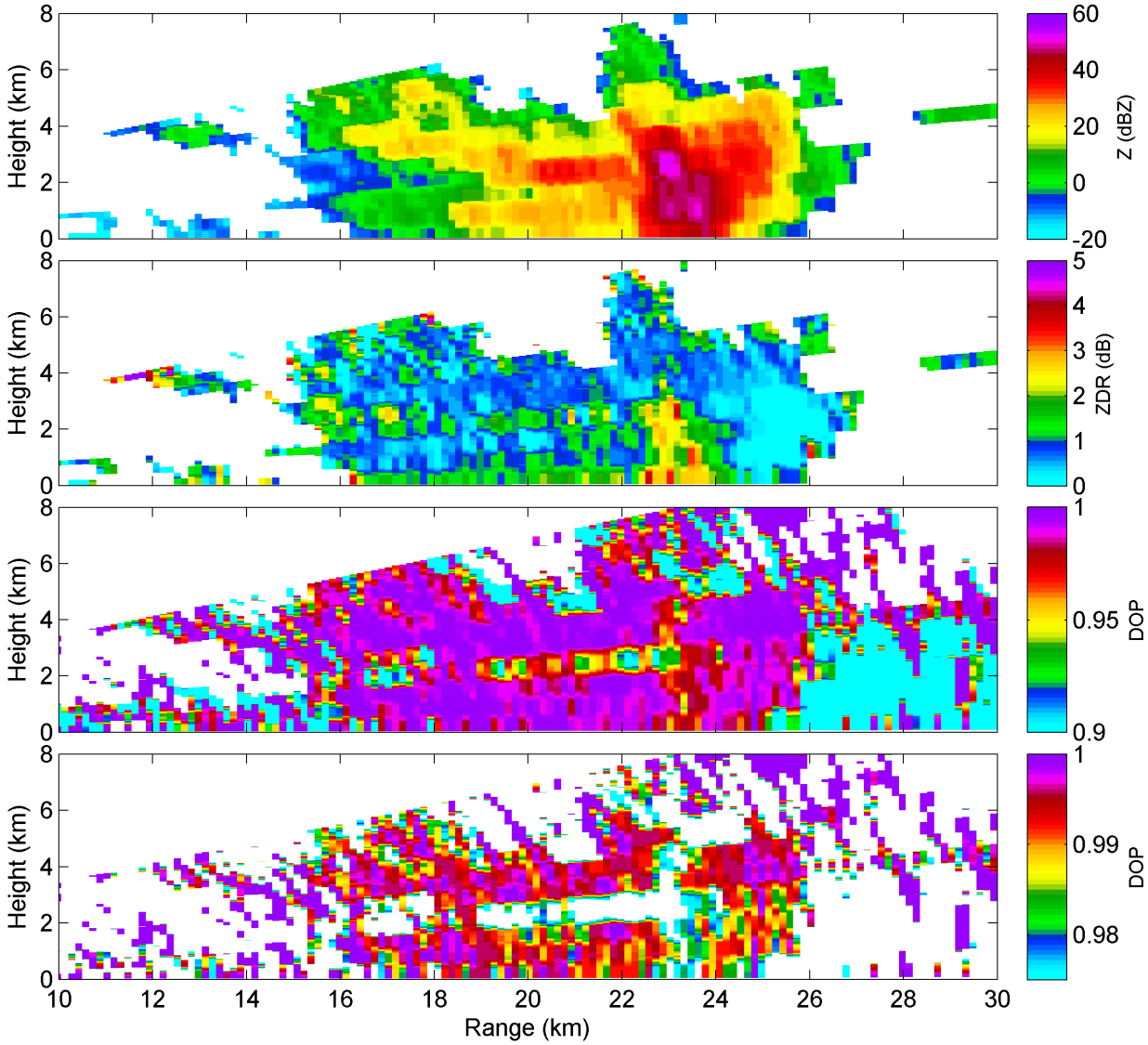

Figure 3: Constructed from PPIs vertical cross-sections of Z_H, ZDR, DOP and a thresholded DOP 1218 on 5 August 2013

5. S*pecific differential phase*, KDP, is derived as follows:

$$KDP = \tfrac{1}{2}\,\Delta\Phi_{DP}/\delta r \quad = \quad \frac{\Phi_{DP}(r_2) - \Phi_{DP}(r_1)}{2\,(r_2 - r_1)} \qquad (2)$$

The factor of ½ accounts for two-way propagation.

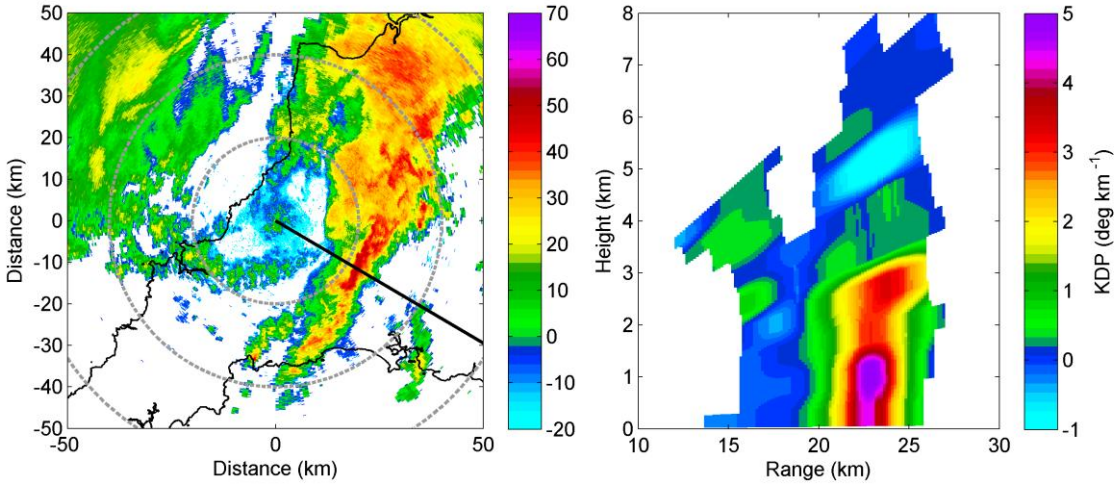

Figure 4: The left hand panel shows the distribution of dBZ at 1218 on 5 August 2013, whereas the right hand panel (K_{DP} deg/km) shows a vertical cut along the line shown on the left hand panel.

Figure 4 shows a PPI of dBZ and a vertical section along the line of the convection of K_{DP} at 1218 on 5 August 2013. Note that negative values of K_{DP} occur above positive values at about 5.5 km altitude. It was suggested by Metcalf (1995) and others that this occurs when hydrometeors have become oriented such that their long axes are approximately in the vertical direction. Ice crystals may assume this vertical orientation when they are subjected to a suitably strong electric field.

Where there are large or partially melting hydrometeors δ can be significant resulting in Mie scattering causing erroneous KDP estimates. Negative values of K_{DP} can occur which may not be completely removed by applying a simple moving average filter and least squares regression to the Φ_{DP} data. Filtering of Φ_{DP} data is essential to obtain suitable input for further dual-polarisation algorithms. In the NCAS radar system the iterative finite impulse (FIR) filter of Hubbert and Bringi (1995) is used. K_{DP} is derived by a least-squares regression of Φ_{DP} over several range gates. The exact number of range gates depends upon the range resolution used. Hence in the case shown in Figure 4 in which a strong electric field is not present the slightly negative values of K_{DP} are probably due to the limitation of the regression and filtering applied in the presence of a few large hydrometeors.

4. Observations of polarimetric variables

Figure 5 shows from the NCAS X-band radar the Z_H PPI, and reconstructed vertical cross-sections of observations of Z_H, Z_{DR} and K_{DP} at 1415 on 2nd August 2013. The vertical cross sections on the 2nd August were taken along the line shown on.

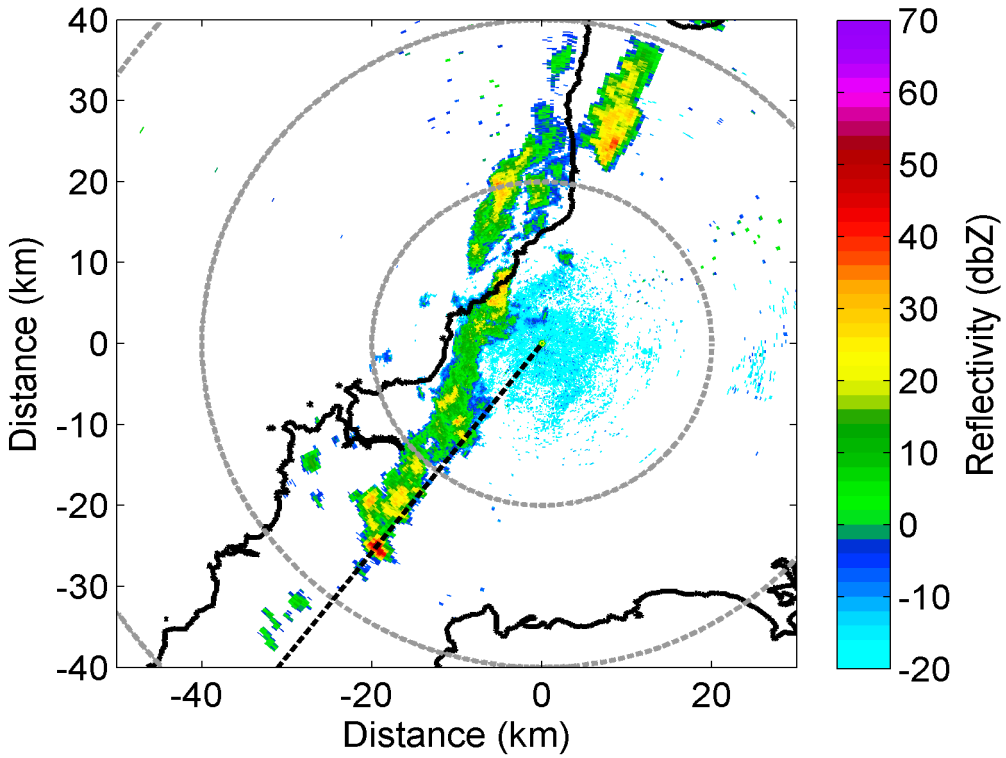

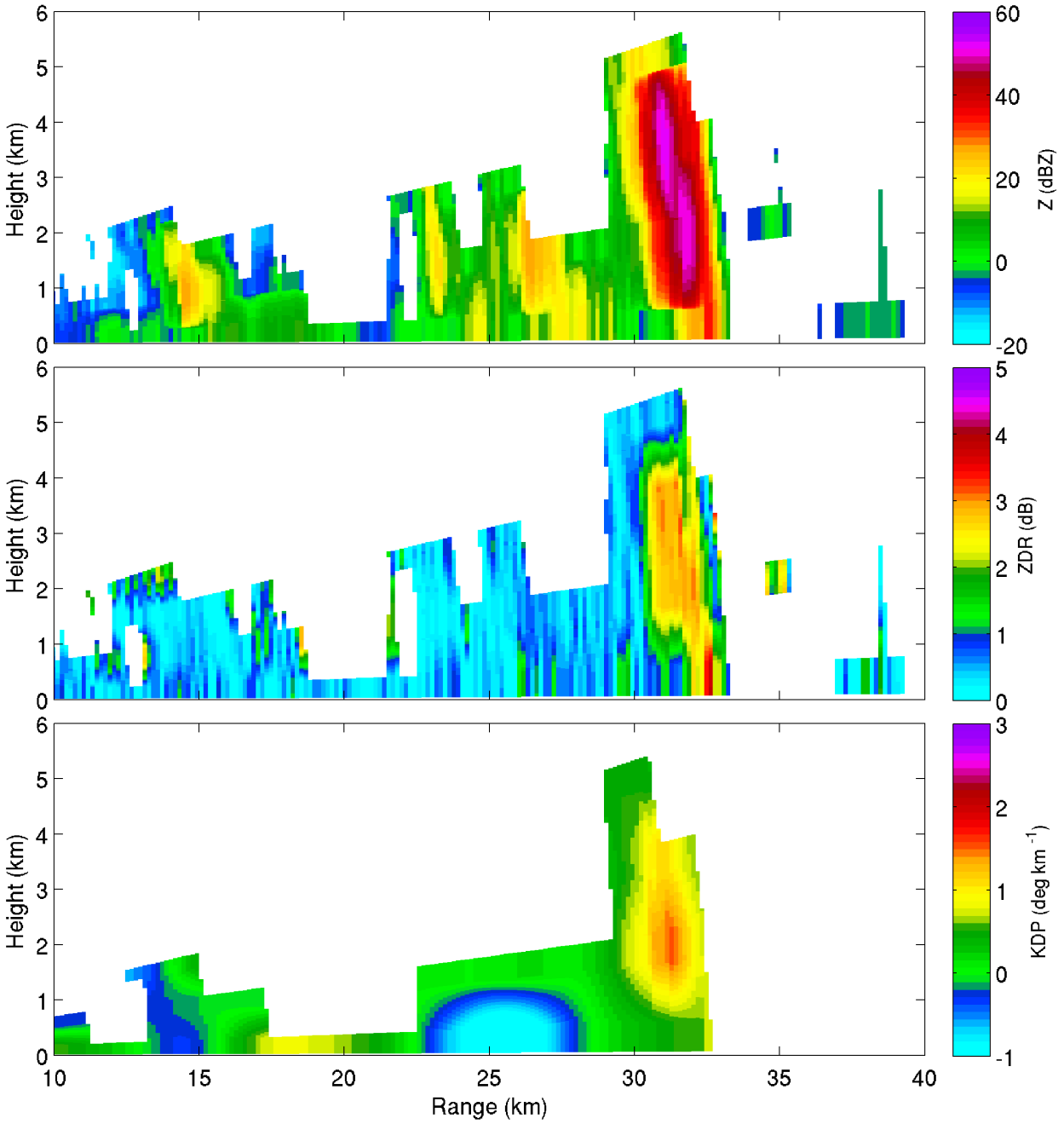

Figure 5: The Z_H PPI, (top panel) and reconstructed vertical cross-sections of Z_H, Z_{DR} and K_{DP} through the line shown on the PPI at 1415 on 2nd August 2013.

the PPI in the top frame of Figure 5. Similar vertical cross-sections are shown in Figure 6. Here the Z_H and Z_{DR} vertical sections for the 3rd August case sections indicate the occurrence of three body scattering, radar-rain-ground-rain-radar, at the far range. This is supported by the values of RhoHV below about 0.6. In Figure 5 and 6 KDP is dependent not only on the shape of the target particles, but on their concentration. For example, low ZDR values, say around 1.5-3dB with elsewhere ZDR values approaching 3 dB indicate that the drops having the larger ZDR values are larger in size than drops having the lower ZDR values. However, when the smaller values of ZDR occur (smaller drops) there may be higher KDP values because the concentration of the drops is higher. The reason for this is the type of process by which the drops are formed as discussed by Blyth et al. (2014). The drops are most likely to be formed via the warm rain process, whereas if the opposite is true a cold rain process is involved.

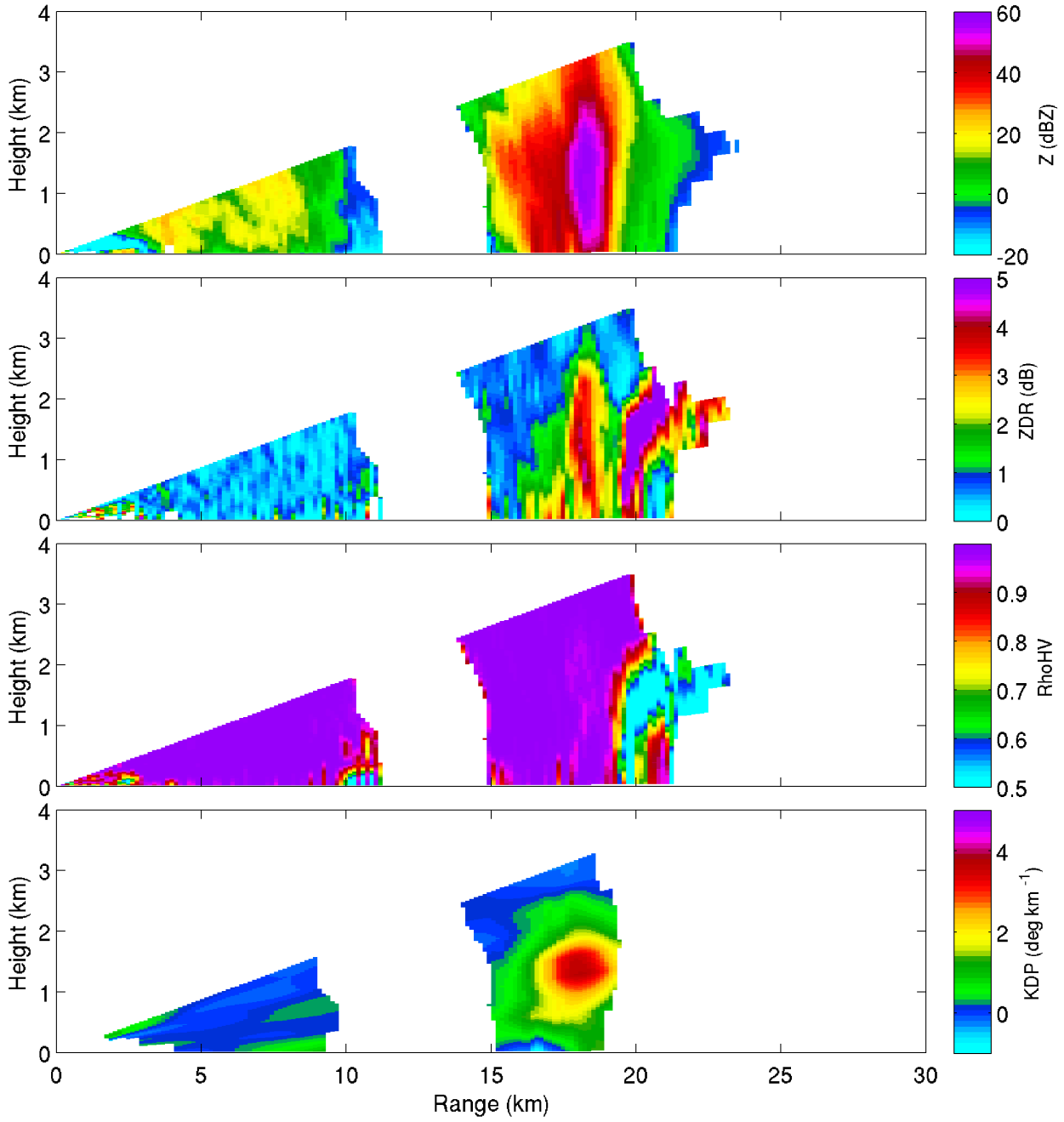

Figure 6: Reconstructed vertical cross-sections of Z_H, Z_{DR}, RhoHV and K_{DP} at 1408 on 3rd August 2013

As mentioned above backscatter from horizontally aligned particles changes the covariances from the values incident upon a scattering volume (Scott et al., 2001) such that

$$\Phi_{HV}|^s = \delta + \Phi_{HV}|^i \quad (3)$$

where δ is the differential phase upon backscatter, and the subscripts i and s denote the incident and scattered values.

$$\Phi_{DP}(r) = \delta(r) + 2\int K_{DP}(s)\,ds = \delta(r) + \phi_{DP}(r) \quad (4)$$

It is clear that the contributions from the backscattered and propagation components of Φ_{DP} need to be separated to confirm whether or not δ is negligible, or whether this has to be taken into account in estimating K_{DP}. In the next section we investigate values of δ observed using the mobile X-band radar.

Note the Z_{DR} columns in both cases and the positive values of K_{DP} occurring next to smaller values of Z_{DR}. In both cases we may estimate δ using the relationship of Schneebeli and Berne (2012),

$$\delta = 0.632\, Z_{DR}^{1.71} \quad (5)$$

Allowing for the calibration mentioned above the values of Z_{DR} at the base of the strong Z_{DR} columns are 2.8 dB on the 2nd August and 3.8 dB on the 3rd August. Hence the corresponding values of δ are about 4.9 degrees. Because δ is immune to

attenuation, it can be used at X-band to quantify mean volume diameters of hydrometeors larger than 2 mm (Tromel et al., 2013). The mass-weighted average raindrop diameter, D_{mw} may be derived from,

$$D_{mw} = a_0 + a_1\delta + a_2\delta^2 \quad (6)$$

Inserting δ = 4.9 deg and taking a_0 = 1.80, a_1 = 0.052 and a_2 = 0.018 at a temperature of 10^0C (Tromel et al., 2013), then D_{mw} = 2.48 mm. Figure 7 shows aircraft measurements of rain drops with diameters greater 2 mm. At a temperature of 0^oC for δ = 4.0 deg D_{mw} = 4.45 mm and for δ = 2.0 deg D_{mw} = 2.05 mm.

The drop median diameter, D_0, may be derived for X-band data from the following formula discussed by Kim et al. (2010) derived from scattering simulations for moderate to heavy rainfall:

$$D_0 = 0.77\ ZDR + 0.79 \quad (7)$$

Taking ZDR as 3.3 dB then D_0 = 3.23 mm. These values of D_0 and D_{mw} may be compared with the aircraft measured drop sizes shown in Figure 7. In this figure drop measurements made with by the University of Wyoming King Air aircraft as it flew along the line shown in Figure 5 are displayed.

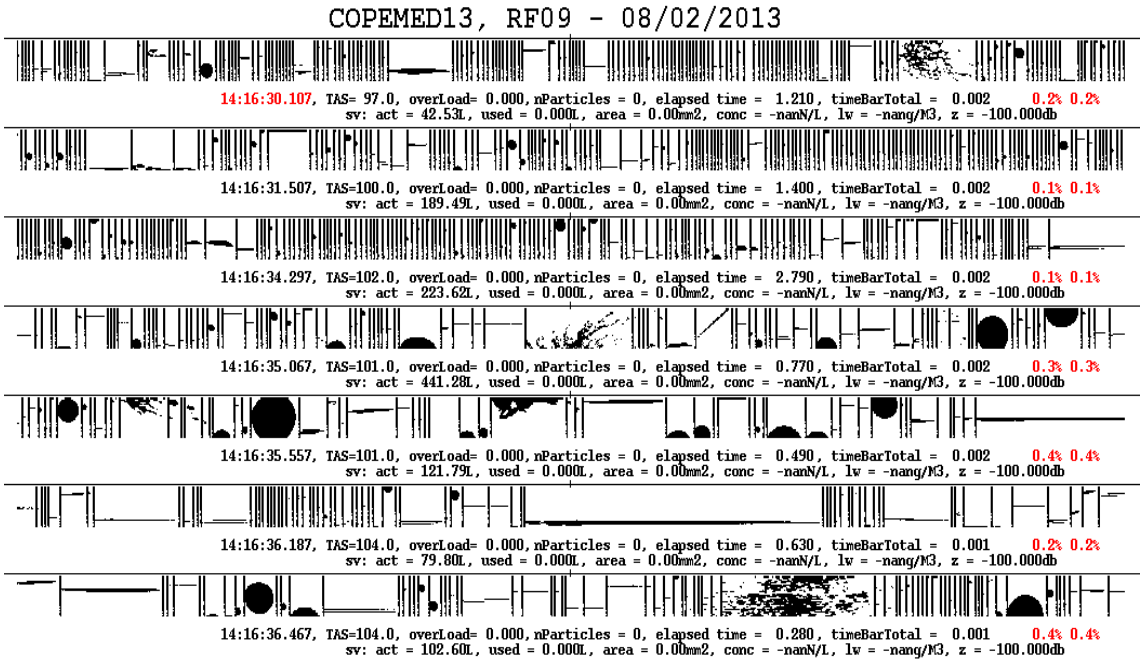

Figure 7: Hydrometeor sizes observed by the University of Wyoming King Air aircraft on the 2nd August 2013 at1416 as it traversed the rain band shown in Figure 5.

Acknowledgement

Thanks are due to all members of the COPE team.

References

Blyth, A., Bennett, L., Collier, C., Huang, Y., Dufton, D. French, J., Brown, P., Choularton, T. and Lean, H. (2014) "Radar and aircraft observations made during COPE of convective clouds force3d by convergence lines in SW of England", this volume.

Doviak, R. J., and D. S. Zrnic (1993) Doppler Radar and Weather Observations. 2nd ed. Academic Press, 562 pp.

Galletti, M. and Zrnic, D.S. (2012) "Degree of Polarization at simultaneous transmit: theoretical aspects", Remote Sensing Letters, IEEE, 9, NO 3, 383-387

Hubbert, J. and Bringi, V.N. (1995) "An iterative filtering technique for the analysis of copular differential phase and dual-frequency radar measurements", J. Atmos. Ocean. Tech., 12, 643-648

Kim, D., -S., Maki, M., and Lee, D., -I. (2010) "Retrieval of three-dimensional raindrop size distribution using X-band polarimetric radar data", J. Atmos. Ocean. Tech., 27, 1265-1285

Metcalf, J.I. (1995) “Radar observations of changing orientations of hydrometeors in thunderstorms”, J. Appl. Met., 34, 757-772

Schneebeli, M. and Berne a. (2012) “An extended Kalman filter framework for polarimnetric X-band weather radar data prcessing”, J. Atmos. Ocean. Tech., 29, 711-730

Scott, R.D., Krehbiel, P.R. and Rison, W. (2001) “The use of simultaneous horizontal and vertical transmissions for dual-polarization radar meteorological observations”, J. Atmos. Ocean. Tech., 18, 629-648

Tromel, S., Kumjian, M.A., Ryzhkov, A.V., Simmer, C. and Diederich, M. (2013) “Backscatter differential phase – estimation and variability”, J. App. Met., 52, 2529-2548